

Integral rate constant measurements of the reaction $\text{H} + \text{D}_2\text{O} \rightarrow \text{HD}(v', j') + \text{OD}$

David E. Adelman, Stephen V. Filseth, and Richard N. Zare

Citation: *J. Chem. Phys.* **98**, 4636 (1993); doi: 10.1063/1.464991

View online: <http://dx.doi.org/10.1063/1.464991>

View Table of Contents: <http://jcp.aip.org/resource/1/JCPSA6/v98/i6>

Published by the [American Institute of Physics](#).

Additional information on *J. Chem. Phys.*

Journal Homepage: <http://jcp.aip.org/>

Journal Information: http://jcp.aip.org/about/about_the_journal

Top downloads: http://jcp.aip.org/features/most_downloaded

Information for Authors: <http://jcp.aip.org/authors>

ADVERTISEMENT



physicstoday

Comment on any
Physics Today article.

Physics Today / Volume 65 / July 2012
Previous Article | Next Article
Measured energy in Japan
David von Seggern
(vonseg@seismo.unr.edu) University of Nevada
July 2012, page 10
DIGITAL OBJECT IDENTIFIER
<http://dx.doi.org/10.1063/PT.3.1619>
The article by Thorne Lay and Hiroo Kanamori is an interesting one. It discusses the energy released by the 2011 Tohoku earthquake. While that of a 100-megaton nuclear explosion is approximately five times as much energy as a 20-megaton nuclear detonation even a 50-megaton atmospheric explosion is approximately five times as much energy as a 10-megaton nuclear device. I believe the authors used the relation for seismic energy release rather than total strain energy release. The seismic energy underestimates the total strain energy release by a variable that depends on friction on the fault plane. Accounting for total strain energy release would increase the earthquake energy number by orders of magnitude. Despite the catastrophic damage potential of nuclear bombs, the forces of nature occasionally unleash much larger energy releases. Although the nuclear bombs are under our control, earthquakes, volcanic eruptions, and extreme weather events are not. However, by judicious preparation and avoidance measures, humans can significantly diminish the damage of natural events.
This article does not have any references.

Comment on this article
By the act of hitting a ball with a bat, one calculates the force energy to deliver the ball to its new location, but one must also take into account that the ball extended its energy release to that which became struck by the ball as its momentum ceased and passed energy to the struck team. Therefore the parameters of the damage extend into the future when the received energy to that pushed upon later becomes released in a new event. Perhaps calculations of one added that in while another's calculations did not. E.M.C.
Written by Edgar McCarvill, 14 July 2012 19:59

Integral rate constant measurements of the reaction $\text{H} + \text{D}_2\text{O} \rightarrow \text{HD}(v', j') + \text{OD}$

David E. Adelman, Stephen V. Filseth,^{a)} and Richard N. Zare
Department of Chemistry, Stanford University, Stanford, California 94305

(Received 30 October 1992; accepted 10 December 1992)

The reaction $\text{H} + \text{D}_2\text{O}$ was studied by intersecting a pulsed beam of HI with an effusive spray of D_2O in a high vacuum chamber. Translationally hot H atoms were generated by UV photolysis of HI in the intersection volume, and the HD product of the reaction $\text{H} + \text{D}_2\text{O}$ was detected in a quantum-state-specific manner by (2+1) resonance-enhanced multiphoton ionization. Because the same UV laser beam was used to initiate the reaction and detect the product, the relative collision energy varied as a function of product state detected— ~ 2.8 eV for $v'=0$, ~ 2.6 eV for $v'=1$, and ~ 2.5 eV for $v'=2$. Under these conditions, approximately 35% of the available energy is partitioned into the internal modes of the HD product. For the products, the HD “new bond” receives 15 times more energy than the OD “old bond.” A significant amount of energy appears as HD vibration with $v'=0$ and 1 having comparable populations. The fraction of available energy partitioned into HD rotation, $g_R(v')$, is found to be essentially independent of HD vibration. This invariance may be rationalized in terms of a counterbalancing of two mechanisms for rotational excitation of the HD product. We find qualitative agreement between recent quasiclassical trajectory calculations by Kudla and Schatz for the HD product internal-state distributions and the present experimental results.

I. INTRODUCTION

In a remarkable series of experiments two decades ago, Polanyi and co-workers¹ used infrared chemiluminescence observations to study simple exoergic bimolecular reactions. These results together with the principle of microscopic reversibility were employed to obtain detailed information about the relative effectiveness of different reactant energy distributions in promoting the reaction in the reverse endoergic direction at the same total energy.^{2,3} The detail of these experimental results has presented a challenge to theoretical reaction dynamics in two areas. The first was the construction of potential energy surfaces of the requisite accuracy and the second was the performance of reactive scattering calculations on these surfaces. The extent to which this challenge has been met can be judged, in part, by the exceptional agreement found between recent experimental and theoretical investigations of the $\text{H} + \text{H}_2$ reaction family.⁴⁻¹¹

The extension of both experiment and theory to the study of atom–triatom bimolecular reactions should lead to an increased understanding of the nature of specific energy requirements for elementary reaction processes. The most promising systems for the comparison of experiment and theory will be of the form $\text{H} + \text{AH}_2 \rightarrow \text{H}_2 + \text{AH}$ because only one of the atoms is electronically complex. Of the first-row AH_2 molecules, BeH_2 and H_2O are closed-shell, chemically stable molecules without low-lying excited electronic states. The former is a high-temperature species posing many technical experimental challenges whereas the latter is readily amenable to study. We may anticipate, therefore, that the study of the endoergic reaction

$\text{H} + \text{H}_2\text{O} \rightarrow \text{H}_2 + \text{OH}$ (and its exoergic reverse reaction¹²⁻¹⁶) should provide the most fruitful comparison between theory and experiment.

The first investigation of specific energy disposal in the $\text{H} + \text{H}_2\text{O}$ reaction was reported in 1984 by Kleinermanns and Wolfrum.¹⁷ They employed translationally hot H atoms produced in the 193 nm photolysis of HBr. The OH “old bond” product of the H-atom abstraction reaction was observed, and little (about 3%) of the available energy was found to appear in rotation. No vibrationally excited OH was produced. Schatz, Colton, and Grant¹⁸ reported approximate agreement with this result in a quasiclassical trajectory (QCT) calculation carried out on a high-quality *ab initio* potential energy surface.¹⁹⁻²¹ Energy disposal has been studied subsequently^{22,23} at other H-atom energies with the conclusion that OH rotational excitation is insensitive to collision energy. Recent investigations of energy disposal in the OD product of the reaction $\text{H} + \text{D}_2\text{O}$ and in the OH and OD products of the $\text{H} + \text{HOD}$ reactions similarly show little excitation of the “spectator” hydroxyl fragment.^{24,25}

Additional product channels for the $\text{H} + \text{H}_2\text{O}$ reaction must be considered. Energy transfer to internal degrees of freedom of H_2O has recently been observed by Lovejoy, Goldfarb, and Leone²⁶ to populate high vibrational levels of the asymmetric stretch. The vibrationally excited H_2O was observed to have preferential in-plane rotational alignment. The authors suggested that this observation implied two possible types of collisions: (1) an approximately collinear and impulsive collision or (2) a “failed-reactive” collision involving a bent planar transition state. The latter type of collision is consistent with QCT calculations²⁷ and theoretical predictions of the H–O–H–H transition-state geometry.¹⁹ Although no experimental information is presently available on the simple exchange reaction, O-atom

^{a)}Department of Chemistry, York University, Toronto, Ontario, Canada M3J 1P3.

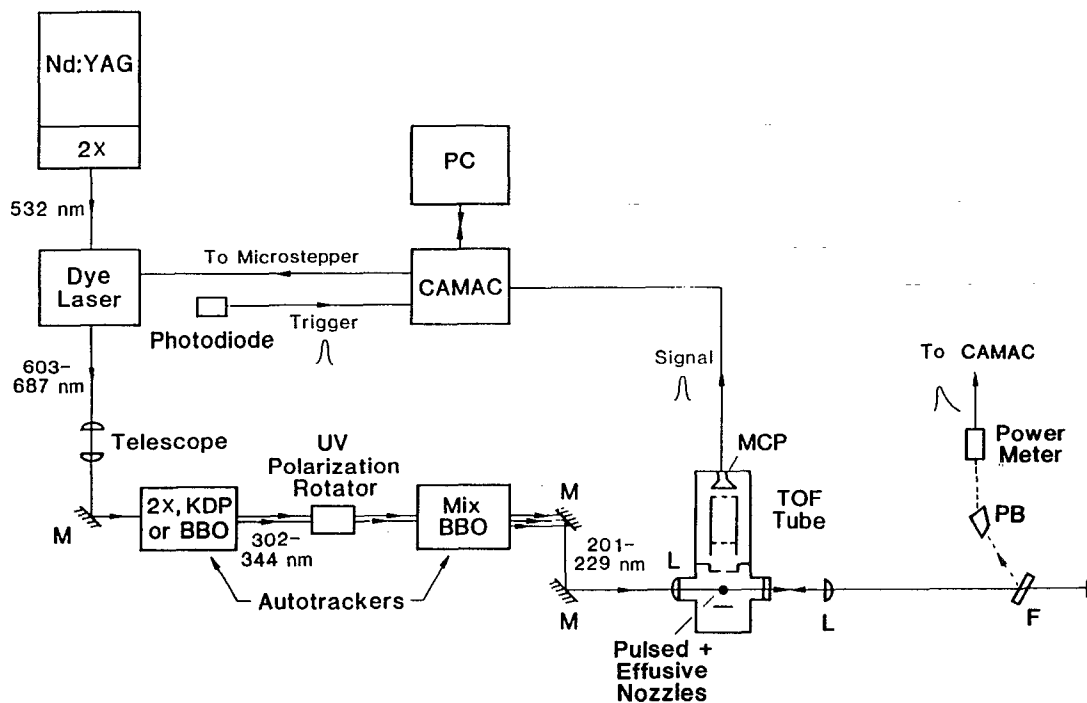


FIG. 1. Schematic diagram of the experimental geometry. M, dichroic mirror; L, lens; PB, Pellin Broca prism, F, BK-7 flat; MCP, multichannel plate detector; and PC, personal computer.

abstraction has been found not to occur in the $\text{D} + \text{H}_2\text{O}$ reaction.²² Recently, the back reaction $\text{OH} + \text{D}_2 \rightarrow \text{HOD} + \text{D}$ has been studied,¹² and the HOD product shows pronounced back scattering, which is consistent with the proposed transition-state geometry.

In addition to these investigations, two groups have reported experimental studies of the effect of vibrational excitation on the abstraction reaction. Crim and co-workers^{28,29} have studied the reactions of thermal H atoms with H_2O and HOD possessing several quanta of vibrational energy. Zare and co-workers^{24,25} have studied the reactions of hot H atoms with HOD and D_2O containing one or two quanta of vibrational energy. These studies have attracted considerable attention because they provide the first examples of bond-specific and mode-selective bimolecular reactions. Corresponding theoretical calculations³⁰⁻³³ have been carried out in an effort to account for the observed reaction cross-section enhancements, OH/OD branching ratio changes, and hydroxyl radical energy disposal arising from vibrational excitation of the water reagent.

In none of the experimental studies mentioned above has observation of the molecular hydrogen coproduct of the abstraction reaction been reported. It is expected that as the "new bond" the molecular hydrogen should receive a greater fraction of the available energy as internal energy than has been observed for the hydroxyl, "old bond." This prediction is supported by the original QCT calculations of Schatz and co-workers¹⁸ for the $\text{H} + \text{H}_2\text{O}$ reaction. In this paper we report measurements of the HD product internal-state distributions for the reaction $\text{H} + \text{D}_2\text{O}$ at a relative

collision energy (E_{rel}) of approximately 2.7 eV; this energy is well above the 0.94 eV (Ref. 34) reaction barrier and far exceeds the reaction's endothermicity (0.66 eV). These results are briefly compared with the QCT calculations of Kudla and Schatz (see the accompanying paper for a more detailed comparison).³⁵ We find that the HD coproduct is both rotationally and vibrationally excited; specifically, approximately 35% of the total energy is partitioned into internal energy of the HD coproduct. In addition, we find that the fraction of available energy partitioned into HD rotation is independent of the HD vibrational state. Excellent qualitative agreement appears to hold between theory and experiment.

II. EXPERIMENT

A. Apparatus

The experimental apparatus and procedure were similar to those used in our studies of the $\text{H} + \text{H}_2$ reaction family.^{5,9} The major modification to the apparatus has been the addition of a second nozzle, which allowed the HI and D_2O reagents to be independently introduced into the chamber.

Figure 1 shows an overview of the experimental setup; the vacuum chamber is detailed in Fig. 2. HI (Matheson; 98.0% stated purity) was purified by a freeze-pump-thaw cycle and mixed with He (Linde, 99.999% stated purity) in the ratio HI:He = 1:2. These reagents were flowed into a high-vacuum chamber via a pulsed, supersonic nozzle (280 Torr backing pressure). Neat D_2O (Aldrich, 99.9% stated purity) was flowed into the chamber via a heated, capillary

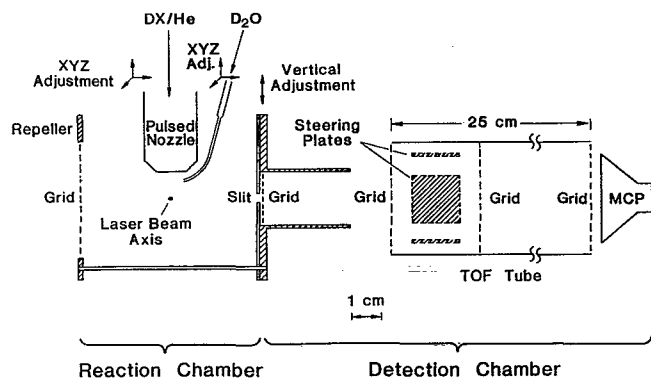


FIG. 2. Expanded view of the reaction and detection chambers.

nozzle. The reagents mixed in the vacuum chamber where the pulsed and effusive reagent beams were crossed (Fig. 2). The reaction was initiated ~ 5 mm below the pulsed nozzle and ~ 2 mm below the capillary nozzle. For these experiments the photolysis/probe laser ($\lambda \approx 210$ nm) photodissociated the HI photolytic precursor and state-specifically ionized the HD reaction product via $(2+1)$ resonance-enhanced multiphoton ionization (REMPI).^{36,37} Because the same laser pulse effected both photolysis and detection, the observed reaction products were formed within the ~ 5 ns pulse duration. The HD^+ ions were detected in a shuttered time-of-flight mass spectrometer (TOF/MS).³⁸

It may be wondered why we did not use an independent photolysis geometry, as in Refs. 39 and 9; such a setup would eliminate the variation in E_{rel} as a function of HD product state detected. We did not pursue this approach because initial experiments showed that the signal-to-noise ratio for the HD product detect was too small. This result is not surprising as the cross section for the $\text{H} + \text{D}_2\text{O}$ reaction is approximately a factor of 4 less than that for the $\text{H} + \text{H}_2$ reaction.

A second nozzle was added to the apparatus because the HI and D_2O reagents react upon being combined in our reagent mixing cylinder. The capillary nozzle (~ 0.5 mm i.d. orifice) was graphite coated and electrically grounded to minimize electrostatic charging. In addition, to eliminate possible clustering of D_2O , the capillary nozzle was resistively heated to 120°C (nichrome wire was wrapped around the nozzle) and the nozzle was fabricated such that the tip tapered very gently. The pressure behind the capillary nozzle was ~ 14 Torr, regulated to $\pm 4\%$ by a needle valve. Under these conditions the flow from the capillary nozzle was effusive. Finally, the position of each of the nozzles could be adjusted independently.

The photolysis/probe laser consisted of a 10 Hz, Nd:YAG-pumped dye laser (YAG denotes yttrium aluminum garnet) (Spectra-Physics, GCR-5, PDL-1) with frequency-doubling and mixing stages (INRAD Autotracker II). The dye laser light was frequency doubled and mixed in β -barium borate (BBO) crystals,⁴⁰ yielding ~ 2.0 mJ per pulse of tunable UV radiation (202–222 nm).

Two dichroic mirrors separated the ~ 210 nm radiation from the other wavelengths and steered the beam into the reaction chamber. A lens mounted on the chamber ($f = 125$ mm) focused the probe beam to approximately $50 \mu\text{m}$ full width at half maximum (FWHM). The probe-laser energy was measured (Moletron J3-09) by taking the back reflection from a Suprasil B flat and passing this light through a Pellin Broca prism to isolate the probe-laser light.

B. HI photolysis

Translationally hot H atoms were generated by UV laser photolysis of HI. The photodissociation of HI results in the production of two groups of H atoms with different speeds, corresponding to the production of ground state $\text{I}(^2P_{3/2}) \equiv \text{I}$ and spin-orbit excited $\text{I}(^2P_{1/2}) \equiv \text{I}^*$. Because HI was photolyzed by the tunable probe laser ($\lambda = 202$ – 221 nm), the photolysis wavelength and therefore E_{rel} varied as different $\text{HD}(v', j')$ levels were detected. The variation in E_{rel} over all rovibrational levels measured [i.e., $\text{HD}(v'=0, j'=3)$ to $\text{HD}(v'=2, j'=11)$] was 3.0–2.4 eV for the fast channel and 2.1–1.5 eV for the slow channel. The variation over a specific vibrational level was (1) 3.0–2.7 eV for the fast channel and 2.1–1.8 eV for the slow channel for $v'=0$, (2) 2.7–2.5 eV for the fast channel and 1.8–1.6 eV for the slow channel for $v'=1$, and (3) 2.5–2.4 eV for the fast channel and 1.6–1.5 eV for the slow channel for $v'=2$. The faster H atoms had a higher collision frequency; thus, their contribution to the measured rates was increased relative to the simple I^*/I ratio. The I^*/I ratio varied as a function of photolysis wavelength.⁴¹ The contribution of the slow H-atom channel to the measured distributions was 12%–20% for $\text{HD}(v'=0)$, 19%–29% for $\text{HD}(v'=1)$, and 27%–32% for $\text{HD}(v'=2)$. Therefore, any complete simulation of the experiment must take into account this variation. To simplify the notation we identify the E_{rel} of the reaction by simply referring to the mean value of E_{rel} for the fast H-atom channel.

C. Experimental checks

1. Interfering reactions

Two possible interfering reactions existed: (1) $\text{H} + \text{DI}$ ($\text{D} + \text{HI}$), derived from the presence of DI in our HI reagent, and (2) $\text{D} + \text{HI}$, where fast D atoms might have been generated from the photodissociation of D_2O . Although the normal isotopic abundance of deuterium is very low, we were running relatively concentrated mixtures of HI in He and, thus, believed that signal from the reactions $\text{H} + \text{DI}$ ($\text{D} + \text{HI}$) could have been significant. The test for this interference was straightforward: we simply flowed the normal HI/He mix through the pulsed nozzle without running the D_2O through the capillary nozzle. We observed no signal from these interfering reactions for any of the rovibrational levels we checked. Based on earlier work,^{42,43} the greatest interference from these reactions would be expected to occur for $\text{HD}(v'=1)$. Thus, we focused our attention on $\text{HD}(v'=1)$, although we did check rovibrational levels in $\text{HD}(v'=0$ and 2) as well; specifically,

HD($v'=0, j'=8, 12, 14$), HD($v'=1, j'=6, 10, 12, 14, 15$), and HD($v'=2, j'=6, 9, 11$) were checked.

Testing for fast D-atom production from the photodissociation of D₂O could only be carried out indirectly. The test involved flowing neat H₂ through the pulsed nozzle and D₂O through the capillary nozzle. We then searched for HD signal from the reaction D+H₂. Although we observed no HD signal for HD($v'=0, j'=3-16$) and HD($v'=1, j'=0-12$), the measurement was complicated by the noise from the large nonresonant signal (i.e., H₂ nonresonant ionization). Because we can discriminate more effectively against higher mass ions with our shuttered TOF/MS we also carried out the same experiment flowing D₂ through the pulsed nozzle and H₂O through the capillary nozzle. Changing to these isotopes did significantly reduce the noise for $m/e=2$. Once again we observed no HD signal at $m/e=3$ for any of the relevant HD($v'=0$ and 1) levels.

We also measured the power dependence of the HD signal for HD($v'=1, j'=7$) and HD($v'=1, j'=12$). If fast D atoms from the photodissociation of D₂O were significant we would have observed a change in the power dependence relative to previous measurements, as the photodissociation of D₂O would entail a two-photon process. A linear least-squares fit to the data gives the laser power dependence, where the population is proportional to the ion signal divided by (laser power)^{*n*}. The power dependence for both levels was approximately $n=1.5$, which is consistent with previous measurements.^{9,37} We are, therefore, confident that fast D-atom production from the photodissociation of D₂O was not significant under the present experimental conditions.

2. D₂O clustering

Because of the high propensity that water exhibits for clustering we were concerned that significant D₂O clustering might occur. This concern led us to use (1) a nozzle in which the pressure drop occurred over a relatively long region of the nozzle and (2) a nozzle that was heated. To test whether we had removed D₂O clustering as a source of systematic error, we varied the temperature of the nozzle and flowed a mix of He and D₂O through the nozzle. The results of these tests are displayed in Fig. 3. We recorded HD internal-state distributions for three capillary nozzle temperatures: 50, 120, and 180 °C. In addition, we flowed a D₂O:He mix of 2.5:1 with a nozzle temperature of 120 °C. All of the distributions are in excellent agreement, thus leading us to conclude that D₂O clustering was not significant under the present experimental conditions.

D. Experimental procedure

We report three sets of HD product rotational distributions in which HI was used to generate fast H atoms. In addition, we determined the vibrational product-state distribution. The H+D₂O → HD(v', j')+OD product rotational distributions were each recorded 12 times on 3–7 separate days. On a given day 1–4 rotational distributions were recorded. Figure 4 presents representative spectral

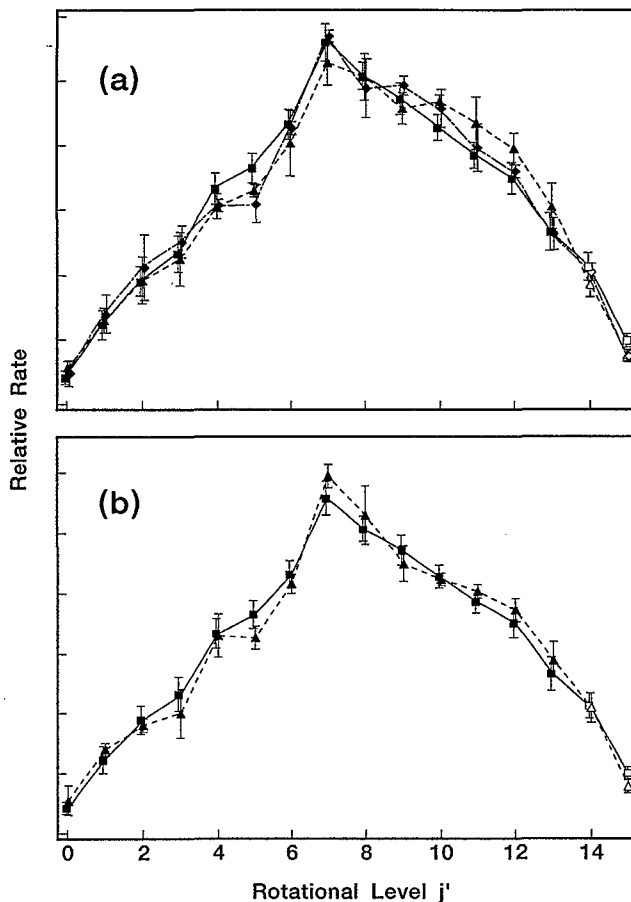


FIG. 3. Comparison of the H+D₂O → HD($v'=1, j'$)+OD at $E_{\text{rel}} \approx 2.6$ eV product rotational distributions: (a) at three different D₂O effusive nozzle temperatures, 50 °C (triangles connected by dashed lines), 120 °C (squares connected by solid lines), and 180 °C (diamonds connected by dash-dot-dashed lines), and (b) flowing neat D₂O (squares connected by solid lines) or a 2.5:1 mixture of D₂O and He (triangles connected dashed lines) at a D₂O nozzle temperature of 120 °C.

peaks for HD($v'=0, 1$, and 2). The peaks displayed in each panel were recorded on a single day; consequently, their areas reflect the relative populations of the rotational levels within a given vibrational state.

Determination of the vibrational product-state distribution entailed relating or “locking” HD($v'=1$) to HD($v'=0$) and HD($v'=2$). Locking two vibrational levels involved measuring the relative rates into a given rotational level in each of the vibrational states. HD($v'=1, j'=12$) and HD($v'=2, j'=4$) were employed to lock $v'=1$ and 2, and HD($v'=1, j'=4$) and HD($v'=0, j'=13$) were employed to lock $v'=0$ and 1. The vibrational levels were locked each day data for $v'=0$ or 2 were recorded.

E. REMPI calibration

The REMPI-TOF/MS detection procedure was calibrated against a high-temperature, effusive nozzle which provided correction factors to convert ion signals into relative populations. The calibration is described in separate publications.^{36,37} Both vibrational and rotational correc-

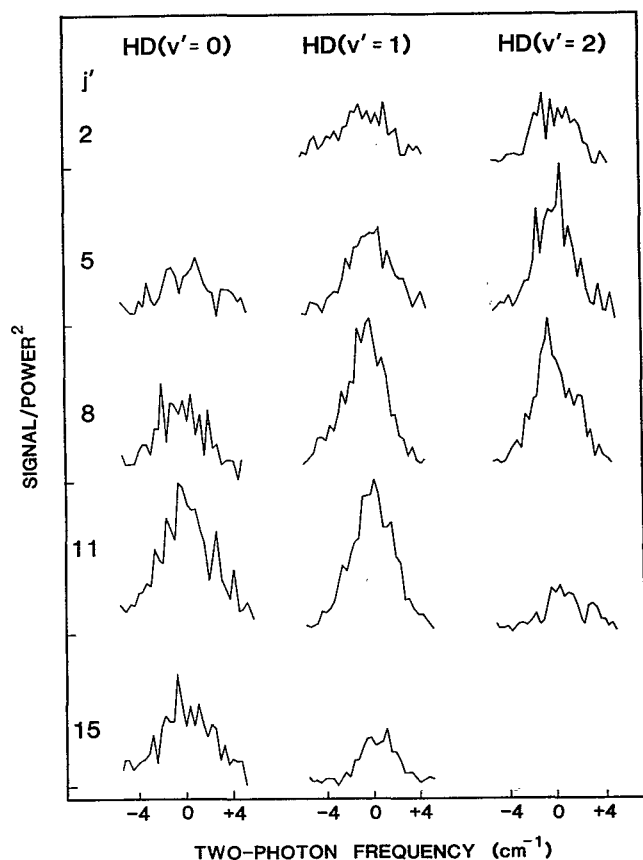


FIG. 4. Representative spectral peaks of the $\text{H}+\text{D}_2\text{O}$ reaction for (a) $\text{HD}(v'=0, j')$ at $E_{\text{rel}} \approx 2.8$ eV; (b) $\text{HD}(v'=1, j')$ at $E_{\text{rel}} \approx 2.6$ eV, and (c) $\text{HD}(v'=2, j')$ at $E_{\text{rel}} \approx 2.5$ eV. Recall, E_{rel} varies as a function of rovibrational state detected and the HI photolytic source produces two groups of H atoms with different speeds (Sec. II B). Each trace represents one scan, which took 90–240 s; see text for additional information on the experimental procedure. All peaks for a given figure were recorded on the same day. On the abscissa, 0 denotes line center.

tion factors were measured; however, the range of calibrated levels does not cover all of the levels measured in these experiments. The HD vibrational levels calibrated were $v=0, 1$, and 2 and the rovibrational levels calibrated were $(v=0, j=0-13)$, $(v=1, j=2-11)$, and $(v=2, j=2-8)$.

Three types of entries appear in Tables I–III and Figs. 1–6.

(1) Calibrated or estimated populations. Calibrated populations use experimentally derived correction factors to relate ion signals to relative quantum-state populations, whereas estimated populations rely on theoretically derived correction factors. For most of these levels the experimentally and theoretically derived correction factors were unity. These levels are denoted by entries in the tables without parentheses (solid squares in the figures).

(2) Uncalibrated populations. For these levels ($j' \geq 14$), significant tunneling occurs in the E, F state, the intermediate state in the $(2+1)$ REMPI detection scheme. The measured ion signals for these levels constitute lower limits on the actual populations. These entries are given in square brackets in the tables (open squares in the figures).

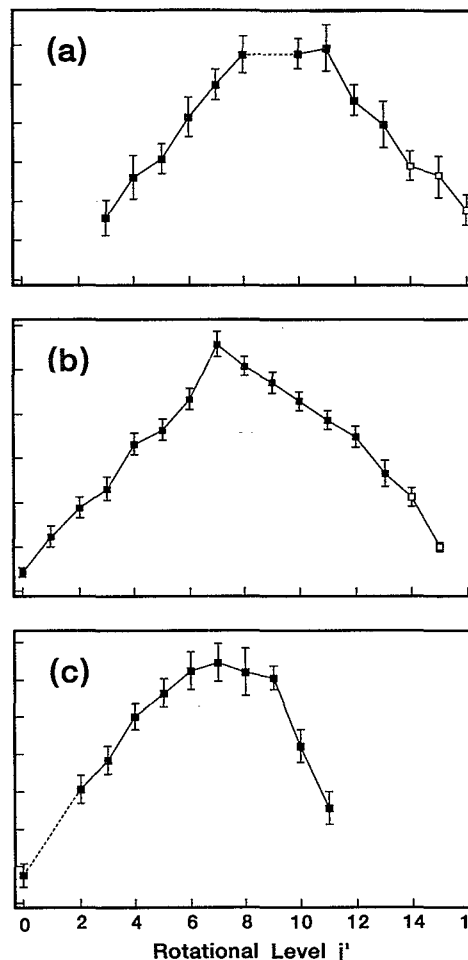


FIG. 5. Rotational distributions of the $\text{H}+\text{D}_2\text{O}$ reaction for the product levels: (a) $\text{HD}(v'=0, j')$ at $E_{\text{rel}} \approx 2.8$ eV, (b) $\text{HD}(v'=1, j')$ at $E_{\text{rel}} \approx 2.6$ eV, and (c) $\text{HD}(v'=2, j')$ at $E_{\text{rel}} \approx 2.5$ eV. Recall, E_{rel} varies as a function of rovibrational state detected and the HI photolytic source produces two groups of H atoms with different speeds (Sec. II B). Error bars represent one standard deviation. Dotted lines connect the populations of levels adjacent to a level for which the population was not measured. Closed markers denote calibrated levels and open markers denote uncalibrated levels.

These levels were included in the normalizations employed to compare the present distributions with theory. They were also used to determine vibrational distributions.

(3) Omitted levels. The $\text{HD}(v'=2, j'=1)$ spectral peak could not be recorded because it overlaps the $\text{HD}(v'=1, j'=15)$ spectral peak in the $(2+1)$ REMPI detection scheme. Similarly, $\text{HD}(v'=0, j'=9)$ and the Lyman β transition for H are in close spectroscopic proximity. As a result of large, interfering ion signals the $\text{HD}(v'=0, j'=9)$ population could not be measured.

III. RESULTS

A. Rotational and vibrational distributions

Rotational product-state distributions have been measured for $\text{HD}(v'=0, 1, \text{ and } 2)$. The rotational distributions are displayed in Fig. 5 and listed in Table I. Error

TABLE I. Product rotational distributions for the reaction H+D₂O → HD(*v'*, *j'*)+OD at $E_{\text{rel}} \approx 2.7$ eV.^a

<i>j'</i>	Relative rate		
	<i>v'</i> =0	<i>v'</i> =1	<i>v'</i> =2
0		0.009±0.002	0.015±0.006
1		0.025±0.004	
2		0.038±0.005	0.061±0.008
3	0.032±0.009	0.046±0.006	0.077±0.008
4	0.05±0.01	0.067±0.005	0.100±0.007
5	0.062±0.008	0.073±0.004	0.113±0.008
6	0.08±0.01	0.086±0.005	0.124±0.01
7	0.100±0.08	0.112±0.006	0.13±0.01
8	0.116±0.009	0.101±0.004	0.124±0.01
9		0.094±0.005	0.121±0.006
10	0.116±0.008	0.086±0.004	0.084±0.009
11	0.12±0.01	0.077±0.004	0.051±0.009
12	0.092±0.008	0.07±0.005	
13	0.08±0.01	0.053±0.006	
14	[0.058±0.008]	0.043±0.004	
15	[0.05±0.01]	[0.02±0.002]	
16	[0.036±0.008]		

^aNote: This is an approximate value because E_{rel} varied as a function of rovibrational state detected and there were two H-atom velocities (see Sec. II B).

bars denote one standard deviation in all figures and tables. The energetically accessible product states are HD($v'=0$, $j'=0-21$), HD($v'=1$, $j'=0-18$), HD($v'=2$, $j'=0-14$), and HD($v'=3$, $j'=0-8$). Therefore, product states are populated quite close to the energetic limit in this reaction. It should be noted that because of the lower detection sensitivity for HD($v'=0$) product states it was not possible to record a complete rotational distribution for $v'=0$. The distributions are all smoothly varying and unimodal, thereby permitting populations of omitted levels to be estimated. Finally, it appears that the peak j' value is relatively insensitive to v' , although there is a slight shift of the peak j' value to lower j' as v' increases.

Determination of the vibrational product-state distribution required two approximations: (1) for the two levels in which measurement was not possible [HD($v'=0$, $j'=9$) and HD($v'=2$, $j'=1$)], populations were determined by linear interpolation between the two adjacent levels, and (2) populations were assumed to be zero for states beyond the range of measured distributions. It is not expected that these approximations affect substantially the calculated values. The vibrational distribution is displayed in Fig. 6 and listed in Table II. The vibrational product-state distribution is relatively "hot," with comparable populations in $v'=0$ and 1.

B. Energetics

Table III summarizes the partitioning of the available energy, E , among the degrees of freedom of the products of the reaction H+D₂O. The available energy is the sum of the relative collision energy, the reagent internal energy, and the reaction endothermicity. The average reagent internal energy was 313 cm⁻¹ for the H+D₂O reaction (the average rotational energy corresponding to D₂O at 300 K).

The first moments, $\langle j' \rangle_{v'}$, and rotational energy partitioning factors, $f_R(v')$ and $g_R(v')$, were calculated for each of the distributions measured, as were the fractions of E partitioned into product vibration and f_V . The formulas used were⁴⁴

$$\langle j' \rangle_{v'} = \sum_{j'} j' P(v', j'), \quad (1)$$

$$g_R(v') = \sum_{j'} P(v', j') E_{v'}(j') / [E - E(v')], \quad (2)$$

$$f_R(v') = \sum_{j'} P(v', j') E_{v'}(j') / E, \quad (3)$$

$$f_V = \sum_{v'} P(v') E(v') / E, \quad (4)$$

where $E_{v'}(j')$ and $E(v')$ are the rotational and vibrational energies, and $P(v', j')$ is the relative population of the HD(v', j') product level and $P(v')$ is the relative population of the HD(v') product level for the reaction H+D₂O → HD(v', j')+OD. The normalizations assumed in Eqs. (1)–(4) are

$$\sum_{v'} P(v') = 1 \quad (5a)$$

and

$$\sum_{j'} P(v', j') = 1. \quad (5b)$$

The approximations described in Sec. III A were used in the above calculations. In addition, the higher E_{rel} associated with the ground-state I channel was used to calculate E . We believe that this is a reasonable approximation because the fast H-atom channel is the dominant channel for HD($v'=0$ and 1) product formation. At the photolysis wavelengths corresponding to HD($v'=2$) product formation, comparable fractions of fast and slow H atoms were

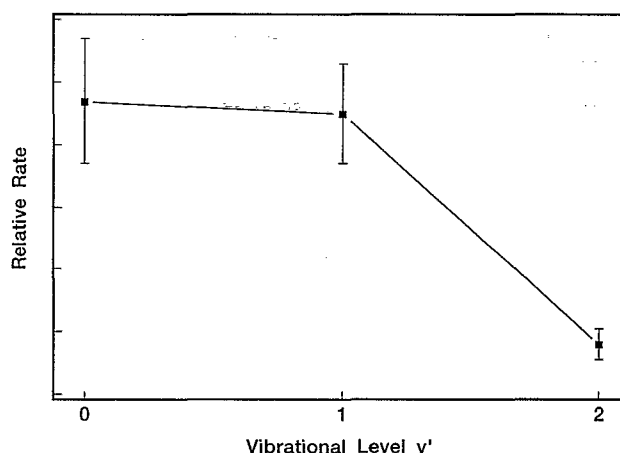


FIG. 6. Vibrational state distribution of the HD product of the H+D₂O reaction at $E_{\text{rel}} \approx 2.7$ eV. Recall, E_{rel} varies as a function of rovibrational state detected and the HI photolytic source produces two groups of H atoms with different speeds (Sec. II B). Error bars represent one standard deviation.

TABLE II. Product vibrational distribution for the reaction H+D₂O → HD(*v'*)+OD at $E_{\text{rel}} \approx 2.7$ eV.^a

<i>v'</i>	Relative population
0	0.47 ± 0.1
1	0.45 ± 0.08
2	0.08 ± 0.02

^aNote: This is an approximate value because E_{rel} varied as a function of rovibrational state detected and there were two H-atom velocities (see Sec. II B).

generated, but the products generated from the slow H-atom channel can only access the lowest rotational levels of HD(*v'*=2). Thus, this approximation remains valid for *v'*=2 as well.

IV. DISCUSSION

A. HD product internal-state distributions

We observe a relatively high degree of internal excitation of the HD product for the reaction H+D₂O, as shown in Figs. 5 and 6 and Table III. Approximately 63% of the available energy appears as translation of the products, given that approximately 2% of the available energy is channeled into the internal modes of the product OD,⁴⁵ 22% into HD rotation, and 13% into HD vibration. An energy-constrained surprisal analysis of the data shows that the data are not fit by a statistical model. Unlike the OD distributions recorded for the reaction H+D₂O,²⁴ we find that the HD distributions cannot be described by temperatures. The OD product's role as a "spectator" is clearly reinforced by these measurements, as the HD product receives 15 times the amount of energy deposited into the OD product.

Perhaps the most intriguing result concerns the fraction of available energy partitioned into HD product rotation, $g_R(v')$. We find that the $g_R(v')$ values for each vibrational level are essentially invariant; see Table III. The fraction of the total energy appearing as HD product rotation, however, does monotonically decrease from *v'*=0 to 1. Thus, there is an energetic constraint on the fraction of energy partitioned into HD rotation derived from the energy taken up in HD vibration. Naively, a corresponding "dynamical constraint" would be expected, based on the

TABLE III. Energy-disposal parameters for the reaction H+D₂O → HD(*v'*, *j'*)+OD at $E_{\text{rel}} \approx 2.7$ eV.^a

<i>v'</i>	$\langle j' \rangle$	f_R	g_R
0	9.3 ± 1	0.26 ± 0.04	0.26 ± 0.04
1	8.0 ± 0.5	0.19 ± 0.01	0.24 ± 0.01
2	6.5 ± 0.6	0.13 ± 0.01	0.24 ± 0.02
All <i>v'</i>	9 ± 2	0.22 ± 0.05	0.25 ± 0.04
$\langle v' \rangle$	0.6 ± 0.2		
f_V	0.13 ± 0.03		

^aNote: This is an approximate value because E_{rel} varied as a function of rovibrational state detected and there were two H-atom velocities (see Sec. II B).

presumption that vibrational excitation of the HD is facilitated by some subset of collisions (e.g., low impact parameter collisions) and that this subset of collisions does not overlap with those that lead to an efficient transfer of reagent translational energy into HD rotation. The present results apparently contradict this simple picture.

We can only speculate on the possible significance of the invariance of $g_R(v')$ with respect to HD vibrational state. It is interesting to note that the same lack of dependence of $g_R(v')$ on *v'* was observed for the H+D₂ reaction at $E_{\text{rel}}=1.3$ eV,³⁹ however, for the D+H₂ reaction⁹ at $E_{\text{rel}} \approx 1.4$ eV $g_R(v')$ was found to vary between the vibrational states. Although this is a very limited set of reactions, an analogy might be drawn to the QCT studies carried out by Kuntz *et al.*⁴⁶ In this set of experiments they designated regions on the PES and then determined in which of these regions energy was partitioned into the internal modes of the reaction products for a series of exothermic exchange reactions (i.e., A+BC → AB+C). They observed a "light-atom anomaly" for reactions of the form L+HH which led to a reduction in $\langle E_{\text{vib}} \rangle$. Using a simple model Kuntz *et al.* suggested that this effect arises because the BC bond does not have time to extend as the light atom approaches. We suggest here that the invariance of $g_R(v')$ may also be attributable to a light-atom effect and that it may be caused by the OD bond not having time to extend as the H atom approaches.

We use the models proposed by Schatz and co-workers¹⁸ to provide a qualitative picture of the rotational dynamics of the H+D₂O reaction. In their paper Schatz and co-workers present two mechanisms for rotational excitation of the HD; rotational excitation of the HD may arise from (1) the instantaneous angular momentum of the OD₂H complex and (2) product repulsion. We make the assumption that, on average, low impact parameter collisions are needed to produce vibrationally excited HD. The instantaneous angular momentum of the system will, consequently, be higher for collisions leading to HD(*v'*=0) than for those leading to HD(*v'*=1 and 2).

The reduction in the system's angular momentum is offset by increased product repulsion for low impact parameter collisions. Product repulsion may be enhanced for low impact parameter collisions because the effective approach velocity of the approaching H atom would be close to its maximum. In contrast, for higher impact parameter collisions the velocity of the H atom only makes a projection along the HD bond axis. Thus, for low impact parameter collisions (vibrationally excited products) the OD bond has little time to extend and the product repulsion is strong, whereas for high impact parameter collisions (vibrationally "cold" products) the OD bond has a relatively longer time to extend and the product repulsion is weak. In other words, the HD vibrational state dictates whether the reagent energy is partitioned on the PES into HD rotation either earlier, little vibrational excitation, or later, significant vibrational excitation. This proposed behavior suggests a simple picture in which the two mechanisms for coupling reagent energy into HD product rotation compete with each other for reactions involving light-atom attack.

B. Comparison with QCT calculations

We provide only a brief summary of the comparison of the present experimental results with the QCT calculations of Kudla and Schatz.³⁵ Please refer to the following paper for a detailed comparison. The QCT calculations take into account the fast and slow H-atom channels; specifically, for each vibrational level they used the mean value of E_{rel} (for the fast and slow channels) and the mean value for the slow channel contribution. We find qualitative agreement overall between the QCT results and experiment. The calculated and measured averaged values $\langle j'(\text{all } v') \rangle$ and $\langle v' \rangle$ agree quantitatively. Agreement between theory and experiment is judged to be good for the vibrational product-state distribution and for the HD($v'=0$ and 1) rotational-state distributions. The QCT HD($v'=2$) rotational product-state distribution, however, is shifted to significantly higher j' relative to that for experiment. The calculated $g_R(v')$ values appear to increase with v' , being $g_R(v'=0)=0.29$, $g_R(v'=1)=0.35$, and $g_R(v'=2)=0.44$. These values contrast sharply with the those of experiment for which $g_R=0.24 \pm 0.02$ for all v' . Further theoretical studies are needed to understand the partitioning of energy into vibration and rotation of the HD product and to determine how features of the PES affect the reaction dynamics.

ACKNOWLEDGMENTS

We thank G. C. Schatz for many useful discussions and for making available to us the results of theoretical calculations prior to publication. The authors would also like to thank N. E. Shafer and H. Xu for experimental assistance. D. E. Adelman gratefully acknowledges the Natural Sciences and Engineering Research Council of Canada for a postgraduate scholarship. This project was funded by the National Science Foundation under Grant No. NSF CHE-89-21198.

- ¹K. G. Anlauf, P. J. Kuntz, D. H. Maylotte, P. D. Pacey, and J. C. Polanyi, *Discuss. Faraday Soc.* **44**, 183 (1967).
- ²J. C. Polanyi and D. C. Tardy, *J. Chem. Phys.* **51**, 5717 (1969).
- ³K. G. Anlauf, D. H. Maylotte, J. C. Polanyi, and R. B. Bernstein, *J. Chem. Phys.* **51**, 5716 (1969).
- ⁴W. H. Miller, *Annu. Rev. Phys. Chem.* **41**, 245 (1990), and references therein.
- ⁵D. A. V. Kliner, D. E. Adelman, and R. N. Zare, *J. Chem. Phys.* **94**, 1069 (1991).
- ⁶M. D'Mello, D. E. Manolopoulos, and R. E. Wyatt, *J. Chem. Phys.* **94**, 5985 (1991).
- ⁷M. Zhao, D. G. Truhlar, and D. J. Kouri, *J. Phys. Chem.* **94**, 7074 (1990).
- ⁸D. Neuhauser, R. S. Judson, D. J. Kouri, D. E. Adelman, N. E. Shafer, D. A. V. Kliner, and R. N. Zare, *Science* **257**, 519 (1992).
- ⁹D. E. Adelman, N. E. Shafer, D. A. V. Kliner, and R. N. Zare, *J. Chem. Phys.* **97**, 7323 (1992).

- ¹⁰D. Neuhauser, R. S. Judson, and D. J. Kouri (unpublished).
- ¹¹Y.-S. M. Wu and A. Kuppermann, *Chem. Phys. Lett.* **201**, 178 (1993); Y.-S. M. Wu, A. Kuppermann, and B. Lepetit, *ibid.* **186**, 319 (1991).
- ¹²M. Alagia, N. Balucani, P. Casavecchia, D. Stanges, and G. Volpi, *J. Chem. Phys.* **98**, 2459 (1993).
- ¹³I. W. M. Smith and R. Zellner, *J. Chem. Soc. Faraday Trans. 2* **70**, 1045 (1974).
- ¹⁴R. Zellner and W. Steinert, *Chem. Phys. Lett.* **58**, 568 (1981).
- ¹⁵A. R. Ravishankara, J. M. Nikovich, R. L. Thompson, and F. P. Tully, *J. Phys. Chem.* **85**, 2498 (1981).
- ¹⁶G. C. Light and J. H. Matsumoto, *Chem. Phys. Lett.* **81**, 578 (1978).
- ¹⁷K. Kleinermanns and J. Wolfrum, *J. Appl. Phys. B* **34**, 5 (1984).
- ¹⁸G. C. Schatz, M. C. Colton, and J. L. Grant, *J. Phys. Chem.* **88**, 2971 (1984).
- ¹⁹S. P. Walch and T. H. Dunning, *J. Chem. Phys.* **72**, 1303 (1980).
- ²⁰G. C. Schatz and S. P. Walch, *J. Chem. Phys.* **72**, 776 (1980).
- ²¹G. C. Schatz and H. Elgersma, *Chem. Phys. Lett.* **73**, 21 (1980).
- ²²K. Honda, M. Takyanagi, T. Hishiyama, H. Ohoyama, and I. Hanazaki, *Chem. Phys. Lett.* **180**, 321 (1991).
- ²³K. Kessler and K. Kleinermanns, *Chem. Phys. Lett.* **190**, 145 (1992).
- ²⁴M. J. Bronikowski, W. R. Simpson, B. Girard, and R. N. Zare, *J. Chem. Phys.* **95**, 8647 (1991); M. J. Bronikowski, W. R. Simpson, and R. N. Zare, *J. Phys. Chem.* (in press).
- ²⁵M. J. Bronikowski, W. R. Simpson, and R. N. Zare, *J. Phys. Chem.* (in press).
- ²⁶C. M. Lovejoy, L. Goldfarb, and S. R. Leone, *J. Chem. Phys.* **96**, 7180 (1992).
- ²⁷G. C. Schatz and H. Elgersma, in *Potential Energy Surfaces and Dynamics Calculations*, edited by D. J. Truhlar (Plenum, New York, 1981).
- ²⁸A. Sinha, M. C. Hsiao, and F. F. Crim, *J. Chem. Phys.* **92**, 4928 (1990).
- ²⁹A. Sinha, M. C. Hsiao, and F. F. Crim, *J. Chem. Phys.* **94**, 4928 (1991).
- ³⁰D.-S. Wang and J. M. Bowman (personal communication).
- ³¹D. C. Clary, *Chem. Phys. Lett.* **192**, 34 (1992).
- ³²K. Kudla and G. C. Schatz, *Chem. Phys. Lett.* **193**, 507 (1992).
- ³³J. M. Bowman and D.-S. Wang, *J. Chem. Phys.* **96**, 7852 (1992).
- ³⁴D. G. Truhlar and A. D. Isaacson, *J. Chem. Phys.* **77**, 3516 (1982); A. D. Isaacson and D. G. Truhlar, *ibid.* **76**, 1308 (1982).
- ³⁵K. Kudla and G. C. Schatz, following paper, *J. Chem. Phys.* **98**, 4644 (1993).
- ³⁶W. M. Huo, K.-D. Rinnen, and R. N. Zare, *J. Chem. Phys.* **95**, 205 (1991).
- ³⁷K.-D. Rinnen, M. A. Buntine, D. A. V. Kliner, R. N. Zare, and W. M. Huo, *J. Chem. Phys.* **95**, 214 (1991).
- ³⁸K.-D. Rinnen, D. A. V. Kliner, R. S. Blake, and R. N. Zare, *Rev. Sci. Instrum.* **60**, 717 (1989).
- ³⁹K.-D. Rinnen, D. A. V. Kliner, and R. N. Zare, *J. Chem. Phys.* **91**, 7514 (1989).
- ⁴⁰The BBO crystal was supplied by R. S. Feigelson and R. K. Route and grown as part of a research program sponsored in part by the Army Reserve Office, Contract No. DAAL03-86-K-0129, and in part by the NSF/MRL Program through the center for Materials Research, Stanford University.
- ⁴¹I. Levy and M. Shapiro, *J. Chem. Phys.* **89**, 2900 (1988).
- ⁴²P. M. Aker, G. J. Germann, and J. J. Valentini, *J. Chem. Phys.* **90**, 4795 (1989).
- ⁴³D. A. V. Kliner, K.-D. Rinnen, M. A. Buntine, D. E. Adelman, and R. N. Zare, *J. Chem. Phys.* **95**, 1663 (1991).
- ⁴⁴R. D. Levine and R. B. Bernstein, *Molecular Reaction Dynamics and Chemical Reactivity* (Oxford University Press, New York, 1980).
- ⁴⁵A. Jacobs, H. R. Volpp, and J. Wolfrum, *Chem. Phys. Lett.* **196**, 249 (1992).
- ⁴⁶P. J. Kuntz, E. M. Nemeth, J. C. Polanyi, S. D. Rosner, and C. E. Young, *J. Chem. Phys.* **44**, 1168 (1966).